U.P.B. Sci. Bull., Series A, Vol. 76, Iss. 3, 2014 ISSN 1223-7027

# PERCOLATION EFFECTS ON DIELECTRIC PROPERTIES OF POLYSTYRENE/BaTiO$_3$ NANOCOMPOSITES

Razvan Florin BARZIC[1], Andreea Irina BARZIC[2], Gheorghe DUMITRASCU[3]

*This work deals with preparation and characterization of polystyrene/barium titanate nanocomposites (PS/BaTiO$_3$). The microstructure changes caused by the formation of the percolation network are evidenced by steady shear and viscoelastic tests. Surface analysis performed by atomic force microscopy confirms the good dispersion and distribution of the BaTiO$_3$ in PS matrix. The dielectric properties are determined both experimentally and theoretically, showing that the high polarizable BaTiO3 network enhances the permittivity from 2.57 to 28, making the studied samples useful for construction of capacitors.*

**Keywords**: barium titanate, ferroelectric ceramics, percolation, nanocomposites.

## 1. Introduction

The actual trend in modern electronic systems consists in development of new active and passive components allowing the minimization of the devices [1]. The technologies regarding the passive parts, like resistors, inductors and capacitors, are continuously evolving. In particular, capacitors are important components in fabrication of flash memories or hard disk drives. This type of memories, are functioning considering the following principle: ferroelectric materials exhibit a net polarization represented by a capacitor, which can be reversed in the presence of an electric field [2]. The asymmetry in the electrical response of ferroelectric materials is also responsible for a lot of instability in the dynamics of circuits whose nonlinear component is a ferroelectric-semiconductor structure. A thin $Bi_4Ti_3O_{12}$ polycrystalline ferroelectric [3] and other ferroelectric type capacitor [4,5] show strong nonlinear dynamics such as period-doubling bifurcation and evolution to chaos induced by the change in the amplitude or frequency of a sinusoidal driving.

Ferroelectric ceramics, such as Pb(Zr,Ti)O$_3$, $CaCu_3Ti_4O_{12}$ or BaTiO$_3$, are the most used compounds for making reliable capacitors. However, they present

---

[1] PhD Student, "Gheorghe Asachi" Technical University, Faculty of Mechanics, Iasi, Romania, România, e-mail: barzicrazvan@tuiasi.ro

[2] PhD, "Petru Poni" Institute of Macromolecular Chemistry, Iasi, Romania, e-mail: irina_cosutchi@yahoo.com

[3] Professor, "Gheorghe Asachi" Technical University, Faculty of Mechanics, Iasi, Romania, România, e-mail: gdum@tuiasi.ro

some drawbacks related to brittleness and high processing temperatures. In this context, many studies [6-8] proposed to overcome these difficulties by incorporation of ferroelectric particles in polymers to obtain micro/nanocomposites exhibiting an optimal balance of properties. The advantage of filler-reinforced polymers is given by their relative ease of processing, good flexibility and dielectric properties.

Among the studied nanocomposite systems designed for high permittivity purposes, $BaTiO_3$ is the most common filler [9]. This compound presents ferroelectric, piezoelectric, and thermoelectric properties. The performance and characteristics of this material is strongly dependent on the size, shape, composition, and morphology of the $BaTiO_3$ particles. On the other hand, polystyrene (PS) is a commercial polymer with high mechanical resistance and good optical and mechanical characteristics [10]. Literature reports few studies on the PS/$BaTiO_3$ system, analyzing the manner in which its dielectric performance is influenced by (1) dehydroxylation of hydrothermal $BaTiO_3$ [11], (2) core-shell structure PS/$BaTiO_3$ [12] and (6) synthesis strategy leading to specific conformations [13]. From the point of view of processing and the pursued application, the preparation method is very important. For this reason, nanocomposite industry often relies on rheological testing since it reveals how the resulting physical properties are affected by the material's microstructure, the particle state of dispersion within the polymer, and the interactions occurring between the filler and the matrix.

In this paper, another approach is employed to prepare PS/$BaTiO_3$ nanocomposites consisting in solution mixing, followed by ultrasonication and hot pressing. Rheological analyses are performed in light of interactions between the $BaTiO_3$ and PS chains or between nanoparticles themselves. The effect of filler loading and dispersion on viscoelastic behavior is examined. In order to understand the relationship between the rheological characteristics and the microstructure of the nanocomposites the dielectric properties are compared to the rheological results.

## 2. Experimental details

The polymer matrix PS, the BaTiO3 nanopowder (with particle size under 100 nm), and the solvent dimethylacetamide (DMAc) are used as purchased from Sigma Aldrich.

The preparation procedure of the PS/BaTiO3 nanocomposites involves the following steps: (1) different amounts of nanoparticles are introduced in glass flasks, each containing 5 ml of solvent; (2) the dispersion of the nanopowder is achieved by ultrasonication with ultrasonic bath model UCI-150 at frequency of 35 kHz and power of 325 W, during 50 min; (3) a fixed quantity of polymer powder is gradually added over the stable nanosuspensions with different percents of $BaTiO_3$ so that the ratio between the continuous and the disperse phase is ranging between 1-30 wt %; (4) the PS/$BaTiO_3$ solutions are homogenized by stirring during 45 min and then deposited on glass substrates; (5) the resulting films are first dried at room temperature in saturated atmosphere of solvent and secondly in vacuum oven at 75°C for 6 h; and (6) the films are compacted by hot pressing at 60°C.

The rheological analyses of the P4VP/AlN nanocomposite solutions are performed on a stress-controlled Bohlin CS50 rheometer, having a measuring system with cone-plate configuration. Shear viscosities are recorded over the 0.01–1000 $s^{-1}$ shear rates, while oscillatory measurements are performed in the frequency range of 0.1 to 60 Hz within the linear viscoelastic regime of the samples (shear stress is fixed at 2 Pa).

Atomic force microscopy (AFM) measurements are performed on a SPM SOLVER Pro-M platform at room temperature.

Dielectric constant is determined using a LCR METER instrument for capacitance measurements. The films with thickness of 50 microns are placed in contact with a capacitor. The measurements are carried out at room temperature at the frequency of 1 MHz.

## 3. Results and discussion

Rheology is useful for controlling of the nanoparticle dispersion quality in liquid matrices. The changes in the microstructure of studied PS/$BaTiO_3$ samples are analyzed by using experimental data from the steady-state shear flow and low amplitude oscillatory shear, combined with rheological models. Figure 1 presents the dependence of apparent viscosity on shear rate, recorded at 60°C, for PS/$BaTiO_3$ solutions containing various percents of nanoparticles. For each analyzed sample the rheological response at low deformation rates is determined by the $BaTiO_3$ dispersion. In order to quantify this result, the following power law expressions are used for fitting the obtained data:

$$\eta = \sigma / \dot{\gamma} = A \cdot \dot{\gamma}^{n-1} \tag{1}$$

where $\eta$ is the shear viscosity, $\sigma$ is the shear stress, $\dot{\gamma}$ is the shear rate, A is a specific preexponential factor and $n$ is the shear thinning exponent (index of flow).

The PS solutions exhibit a Newtonian behavior in the entire domain of applied shear rates. The matrix behavior is the same for different temperatures, but in Figure 1 is exemplified the experiment realized at the temperature for which the pressing of the films was performed. The PS/$BaTiO_3$ nanocomposite solutions are characterized by an increase of apparent viscosity, which becomes dependent on the shear rate. It can be noticed that the Newtonian regime is reduced as the nanofiller amount is higher, while the thinning behavior becomes more pronounced.

The index of flow is determined, at a given $BaTiO_3$ percent, by fitting the logarithmic $\sigma = \sigma(\dot{\gamma})$ curve at the lowest shear rates with the dependence expressed by equation (1). At $\dot{\gamma} < 5\ \mathrm{s}^{-1}$, the rheological response is prevalently represented by the nanofiller structure in the composite. The shear thinning exponent is evaluated from the slope of the flow curves plotted in Figure 2. The inset graph represents the variation of flow index with the nanofiller amount.

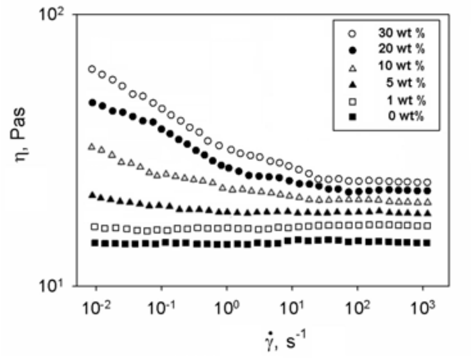

Fig. 1. Apparent viscosity dependence on shear rate for $PS/BaTiO_3$ solutions at 60°C.

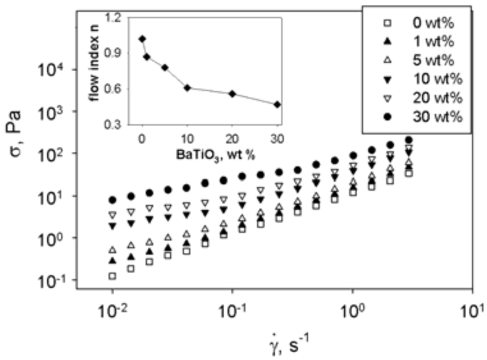

Fig. 2. Shear stress *versus* shear rate for $PS/BaTiO_3$ solutions at 60°C.

The flow index values of $PS/BaTiO_3$ are ranging from 1.02 to 0.46. A flow index close to unity is indicative of a Newtonian flow system. If the reinforced samples behave as the polymer matrix, essentially Newtonian, they are usually not nanocomposites, and such behaviour reveals the presence of micrometer size aggregates. In contrast, nanocomposites demonstrate a considerable shear thinning (n<1) at a relatively small filler volume fraction, and thus usually comprise the morphology of smooth, finely dispersed nanoscale filler. Additionally, samples with moderate values of n (around 0.5 or lower) are very good dispersed in the polymer [14]. As seen in the inset graph from Figure 2, the studied materials exhibit low flow indices, indicating that the $BaTiO_3$ nanoinclusions are well dispersed in PS.

The sudden change in the flow properties of the samples means that the studied nanocomposites have reached rheological percolation at which the $BaTiO_3$ nanoparticles impede the motion of PS chains. This behavior is also reflected in the viscoelastic properties of the samples, expressed through the dependence of storage, G', and loss, G'', moduli on angular frequency, $\omega$, of the investigated solutions. Since the parameter G' is more sensitive to the changes in the sample elasticity in Figure 3 is represented its dependence on $\omega$. The pure PS exhibits terminal behavior similar to linear polymers with scaling properties of approximatively $G' \propto \omega^2$ and $G'' \propto \omega^1$. The power law dependence of both rheological moduli on angular frequency weakens monotonically with increasing AlN loading, especially at low angular frequencies. This result suggests that the nanoparticles not only cause the restriction of PS chain relaxation, but also influence the short-range dynamics or local motion of polymer chains in the nanocomposites. Therefore, a transition from viscoelastic liquid to solid-like behavior takes place as a result of the enhancement of the nanoparticle-nanoparticle interactions, leading to a percolation network.

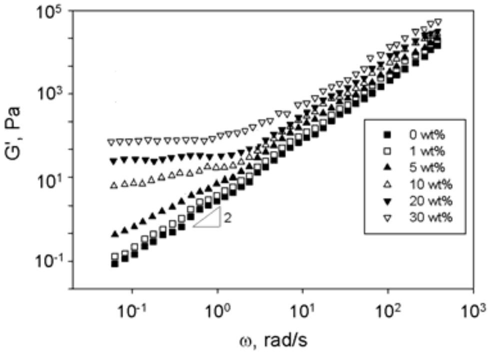

Fig. 3. Dependence of the storage modulus on angular frequency for PS/BaTiO$_3$ solutions at 60°C.

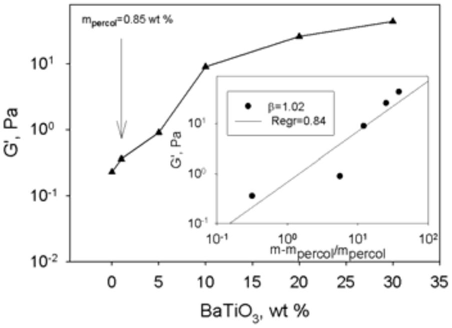

Fig. 4. Storage modulus dependence on nanoparticle loading at 1 rad/s for PS/BaTiO$_3$ solutions at 60°C.

The nanocomposite solutions show an increase in the storage modulus with increasing the reinforcement degree. The sudden modification in the sample's microstructure can be analyzed using a power law to determine the threshold of the rheological percolation:

$$G' \propto \left(m - m_{percol}\right)^{\beta} \tag{2}$$

where $m$ is the nanofiller mass fraction, $m_{percol}$ is the threshold of the rheological percolation and $\beta$ is the critical exponent.

When the shear angular frequency is fixed a power law dependence of G' on the BaTiO$_3$ loading exists for the analyzed samples (see Figure 4). At $m_{percol}$ =0.85 wt % the storage modulus begins to increase from 0.23 to 0.39.

The effect of BaTiO$_3$ reinforcement is also examined by atomic force microscopy. Figure 5 shows the morphology of both continuous and disperse phases. The pure polystyrene film, which is not subjected to hot pressing, exhibits a surface with pores. The parameters characterizing the surface are influenced by the processing technique [15]. For PS sample, the root mean square (RMS) parameter is about 186 nm. Addition of ceramic nanofillers changes the surface features of the matrix, and application of the hot pressing process leads to films without pores.

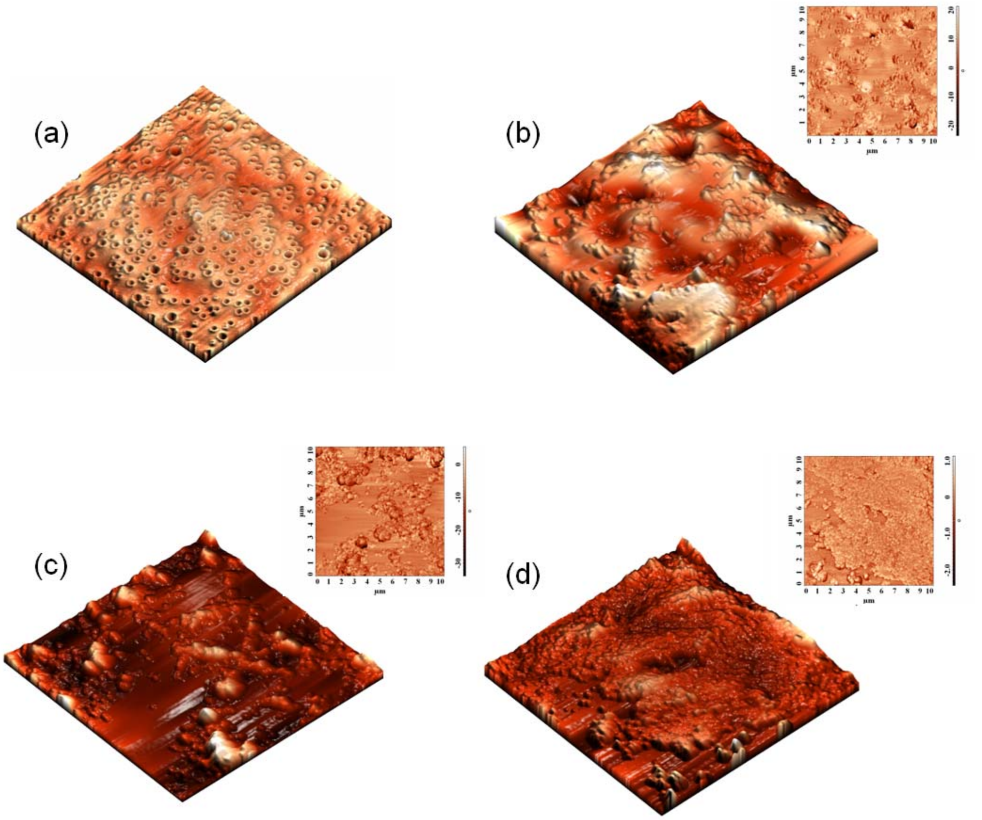

Fig. 5. Atomic force microscopy images of studied films (a) PS without hot pressing at 60°C, (b) 5 wt %, (c) 10 wt % and (d) 30 wt % nanoparticles.

For all $BaTiO_3$ reinforced films AFM images show that the nanoparticles are well dispersed in the matrix, while the phase images confirm the good distribution of the nanoparticles. The RMS is decreasing from 150 nm at 5 wt %, to 123 nm at 10 wt % and to 50 nm at 30 wt % $BaTiO_3$. The reduction of this parameter is explained by considering the fact that with increasing the loading more nanoparticles are positioned at the nanocomposite surface and less polymer-filler bumps are formed. Moreover, it can be noticed that by increasing the $BaTiO_3$ content the nanoparticles are brought more closely one to another and they form a solid-like percolation network. This aspect is more pronounced at the highest concentration of 30 wt %, being favorable for enhancing certain properties required in some microelectronic applications, in particular the dielectric characteristics. The introduction of high polarizable $BaTiO_3$ in PS will result in an enhancement of the dielectric properties of the system. High permittivity materials are often used as embedded capacitors. They represent the primary way of further miniaturizing electronic systems because the ratio of capacitors to the total passive components can be as high as 60 %. However, for these applications the relative dielectric constant must be higher than 4.

The dielectric constant, $\varepsilon$, of PS/$BaTiO_3$ is evaluated from the electrical capacitance data, according to equation (3):

$$\varepsilon = \frac{C \cdot d}{\varepsilon_0 \cdot S} \tag{3}$$

where $d$ and $S$ represent thickness and area of the sample, $C$ is the capacitance and $\varepsilon_0$ represents the absolute permittivity.

The variation of experimental dielectric constant as a function of ceramic inclusions percent is shown in Figure 6. Several theoretical models, such as Maxwell-Garnett (equation (4)), Lichtenecker (equation (5)) and Vysotsky (equation (6)) are used to correlate the permittivity of the ceramic dispersed polymer nanocomposites.

$$\varepsilon = \varepsilon_m \frac{2(1-\phi_p)\varepsilon_m + (1+2\phi_p)\varepsilon_p}{(2+\phi_p)\varepsilon_m + (1-\phi_p)\varepsilon_p} \tag{4}$$

$$\varepsilon = \varepsilon_m^{\Phi_m} + \varepsilon_p^{\Phi_p} \tag{5}$$

$$\varepsilon = \varepsilon_p (\varepsilon_{percol} / \varepsilon_p)^{(1-\phi_p / 1-\phi_{percol})^{n_p}} \tag{6}$$

where $\varepsilon_p$ is the dielectric constant of the particle and $\varepsilon_m$ is the dielectric constant of the the matrix; $\phi_p$, $\phi_m$ and $n_p$ represent the volume fractions of the particles, polymer and percolation network exponent.

Regarding the experimental values, one can distinguish two regions with different slopes in the measured values of $\varepsilon$, as the $BaTiO_3$ percent in system increases. These two points can be correlated with the microstructure modifications, denoted by the flocculation and percolation thresholds. Thus, in the low concentration domain of nanoparticles (1-5 wt%) a slightly linear increase of the dielectric constant is observed. At 0.89 wt% the slope is changed owing to the increase of the particle-particle interactions in the samples resulting in flocculation (fractal flocs). Similarly to viscoelastic properties, at this point takes place the formation of a structure dominated by uniform $BaTiO_3$ agglomerates which penetrate the polymer continuous phase. Further addition of nanofiller in PS determines another increase of the slope at 4.79 wt% indicating that within the polymer the fractal flocs are long-range connected, constituting a three-dimensional (network) supramolecular structure. The microstructural modifications in the studied materials generate non-linear augmentation of the dielectric constant (in regard with the matrix) due to the formation of a high polarizable network of $BaTiO_3$.

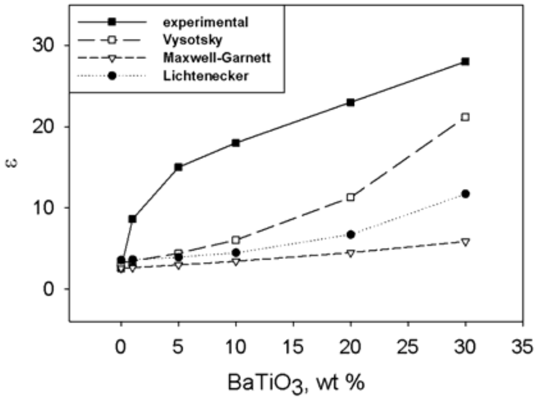

Fig. 6. The dependence of dielectric constant on nanofiller percent for PS/$BaTiO_3$ samples.

There are some discrepancies between the measured values and those calculated with equations (4)-(6). The percolation model proposed by Vysotsky leads to closest values to the experimental ones. According to this approach at a critical nanoparticle percent of 0.89 wt % the dielectric constant increases from 2.57 to 3.46, and the corresponding percolation network exponent is of 0.97.

Comparatively with the rheological percolation threshold, the value corresponding to the dielectric constant is slightly higher. This percolation threshold is reached when a filler network is formed. A polarizable "infinite" path or cluster is sufficient to obtain a high permittivity composite. However, when this threshold is achieved the amount of filler is high enough to significantly affect the elasticity/rigidity of the polymer matrix. Fewer nanoparticles are needed to form a $BaTiO_3$ network inside the PS matrix.

The formation of a percolated structure favors the accumulation of electric charge around the $BaTiO_3$ nanoparticles thus enhancing dielectric constant values. Therefore, the nanocomposite material is able to store more electrical energy by an applied voltage – property required for construction of electronic passive components. This type of materials with relatively high dielectric constant can be used in electronic packaging.

## 4. Conclusions

New nanocomposites are prepared from PS and $BaTiO_3$ nanoparticles, using solution mixture technique, followed by ultrasonication and hot pressing. The sudden changes recorded in the shear thinning index reflect a good dispersion of the nanofiller in the polymer. Also, the response of storage modulus at low angular frequencies reflects the formation of a percolated structure. The AFM data indicate a decrease of RMS parameter and the formation of a nanofiller pseudo-network with increasing the amount of BaTiO$_3$. The introduction of the ceramic nanoinclusions leads to the enhancement of the composite permittivity, particularly at high loading, recommending the studied samples as candidates for construction of capacitors.

## Acknowledgements

This paper was realized with the support of POSDRU CUANTUMDOC "Doctoral Studies for European Performances in Research and Innovation", ID79407, project funded by the European Social Fund and Romanian Government.

## REFERENCES

[1] *M. Nicolaidis*, Soft Errors in Modern Electronic Systems, Editura Springer, London, 2011.
[2] *J.F. Scott,* Ferroelectric memories, Springer Verlag, Berlin, 2000.
[3] *C. Stan, B. Mereu, C. P. Cristescu, A. Lupascu,* "3D analysis of the dynamics of a metal-ferroelectric-semiconductor heterostructure", *Proc. SPIE* 5972, Advanced Topics in Optoelectronics, Microelectronics, and Nanotechnologies II, 59721D, 2005.
[4] *C.P. Cristescu, B. Mereu, C. Stan, M. Agop,* "Feigenbaum scenario in the dynamics of a metal–oxide semiconductor heterostructure under harmonic perturbation. Golden mean criticality." *Chaos, Solitons and Fractals* **vol 40,** 2009, pp. 975-980.
[5] *B. Mereu, M. Alexe, M. Diestelhorst, C.P. Cristescu, C. Stan, "*Investigations on the dynamics of a metal-ferroelectric-semiconductor heterostructure", J. of Optoelectronics and Advanced Materials, **vol 7**, 2005, pp. 691-695.
[6] *N. Gopi Devaraju, E. S. Kim, B. I. Lee*, "The synthesis and dielectric study of BaTiO3/polyimide nanocomposite films", in Microelectronic Engineering, **vol. 82**, 2005, pp. 71–83.
[7] *E.P. Gorzkowski, M.J. Pan*, "Barium titanate-polymer composites produced via directional freezing", in IEEE Trans Ultrason Ferroelectr Freq Control., **vol. 56**, 2009, pp. 1613-1616.
[8] *Z.-M. Dang, Y.-H. Lin, C.-W. Nan*, "Novel Ferroelectric Polymer Composites with High Dielectric Constants", in Advanced Materials, **vol. 15**, 2003, pp. 1625–1629.
[9] *L. Stoica, F. Bygrave, A.J. Bell, "*Barium titanate thin films for novel memory applications", in U.P.B. Sci. Bull., Series A, **vol. 75**, 2013, pp. 147-158.
[10] *N.M. Foote*, "Thermoplastic Flow of Polystyrene", in Ind. Eng. Chem., **vol. 36**, 1944, pp. 244–248.
[11] *P. Badheka, V. Magadala, N.G. Devaraju, B.I. Lee, E.S. Kim*, "Effect of dehydroxylation of hydrothermal barium titanate on dielectric properties in polystyrene composite", in J. Appl. Polym. Sci., **vol. 99**, 2005, pp. 2815-2821.
[12] *K. Yang, X. Huang, L. Xie, C. Wu, P. Jiang, T. Tanaka*, "Core-shell structured polystyrene/BaTiO3 hybrid nanodielectrics prepared by in situ RAFT polymerization: a route to high dielectric constant and low loss materials with weak frequency dependence", in Macromol. Rapid Commun., **vol. 33**, 2012, pp. 1921-1926.

[13] *H.Z. Guo, Y. Mudryk, M.I. Ahmad, X.C. Pang, L. Zhao, M. Akinc, V.K. Pecharsky, N. Bowler, Z.Q. Lin, X. Tan*, "Structure evolution and dielectric behavior of polystyrene-capped barium titanate nanoparticles", in J. Mater. Chem., **vol. 22**, 2012, pp. 23944-23951.

[14] *R. Kotsilkova*, Thermoset Nanocomposites for engineering applications, Editura Smithers Rapra Technology Limited, Shawbury, 2007.

[15] *I. Stoica, A.I. Barzic, C. Hulubei*, The impact of rubbing fabric type on surface roughness and tribological properties of some semi-alicyclic polyimides evaluated from atomic force measurements, in Appl. Surf. Sci., **vol. 268**, 2013, pp. 442-449